2

Elementary Penetration Theory

2.1 Introductory Comments

This chapter is intended to provide a qualitative understanding of the stopping and scattering of charged particles in matter and to acquaint the reader with some of the problems to be solved and suitable tools for their solution. Most of the actual estimates given for specific quantities will be improved or generalized in later chapters. This should not keep the novice from going rather carefully through the material.

The ideas described here have been developed early in the past century to describe the penetration of alpha and beta particles through matter. They have since then been applied to a much wider variety of particles at higher and lower energies than those accessible with the products of natural radioactive decay.

In order to appreciate the validity of the approach taken, have a look at a classical cloud-chamber photograph of the trajectories of alpha particles in air, Fig. 1.1 on page 4. The trajectories are essentially straight lines of almost equal length, of the order of a few centimeters in a gas at atmospheric pressure. Once in a while a trajectory is observed to be bent. Although the process of stopping and scattering is the result of the interaction of the alpha particle with a great number of atoms and therefore must be a statistical process, statistical fluctuations seem to be small and angular deflections rare in the case depicted in Fig. 1.1.

In this chapter, unless otherwise stated, general theoretical considerations are illustrated on an alpha particle moving through a layer of gas that is much thinner than the total length of the trajectory, essentially along a straight line and with very small variation in velocity. Basic concepts introduced include cross section, stopping force and straggling, range, single and multiple scattering, and others. Estimates of these quantities will be based on classical mechanics, much in the way performed in early studies in this field (Rutherford, 1911, Thomson, 1912, Darwin, 1912, Bohr, 1913, 1915).

2.2 Collision Statistics

2.2.1 Definition of Cross Section

The concept of a cross section is of paramount importance in all penetration theory. It is appropriate, therefore, to spend some time on ways of defining and determining this parameter.

Macroscopically the cross section of a target is the area within which it can be hit by some bullet. For example, a spherical target with a radius a offers a cross section πa^2 to a point projectile.

Microscopically we have to come to an agreement on what to mean by saying that a target has been hit by a projectile. In view of the great variety of possible projectiles and targets it is desirable to find a broad definition. Let us say that a target has been hit if the interaction of the projectile with the target has had some specific measurable effect. This means that the magnitude of a given cross section does not only depend on the target, the projectile, and their relative velocity, but also on the physical effect that we decided to monitor. Consequently we talk about scattering cross sections, absorption cross sections, energy-loss cross sections, ionization cross sections, cross sections for specific nuclear reactions, and many others.

Most often in penetration phenomena, the target is an atom or a molecule. In the present chapter we shall also refer to nuclei and/or electrons when talking about targets.

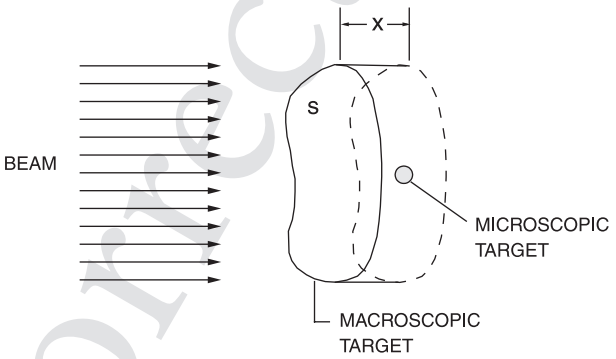

Fig. 2.1. Statistical definition of a cross section: One microscopic target bombarded by a beam

For fundamental and practical reasons there is no way of experimentally determining microscopic cross sections by bombarding one atom with one projectile only. Instead we utilize the statistical information extracted from a large number of bombardments. In that context, we talk about the *stopping medium* and the *beam*. A stopping medium consists of a macroscopic number

of target particles in some arbitrary configuration, such as a random assembly of molecules in an ideal gas or a regular structure of atoms in a crystal. A beam consists of a large number of projectiles. Ideally, all projectiles have the same initial state and velocity, but this is not a necessary requirement. We may also talk about a beam when dealing with alpha or beta particles emitted isotropically from a radioactive source. More important is the initial requirement that *individual projectiles only interact with the stopping medium and not with each other*; this can be achieved by letting individual bombardments be well separated in time. In other words, we consider penetration phenomena in the limit of low beam current here.

Let some microscopic target be bombarded by a beam of projectiles spread homogeneously over an area S (Fig. 2.1). If σ_A is the cross section for some process A – such as ionization of the projectile particle – then, σ_A/S is the fraction of all projectiles that undergo the process A by interacting with the target particle, provided that the number of projectiles is large enough to make statistical fluctuations vanishingly small.

If the beam has a current density J [projectiles/time/area], then

$$J\mathsf{S} \times \frac{\sigma_A}{\mathsf{S}} = J\sigma_A \tag{2.1}$$

is the number of events A induced by the beam per unit time.

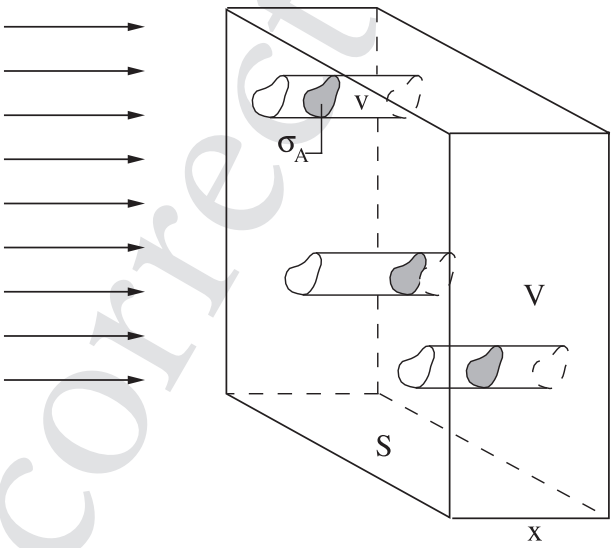

Fig. 2.2. Macroscopic target consisting of randomly placed microscopic targets at number density N, bombarded by a beam

Consider next a stopping medium with a number density N [targets per volume] within a volume $V = \mathsf{S}x$ (Fig. 2.2). According to (2.1) the number of events A induced per unit time by the beam is given by

$$N \times \mathsf{S}x \times J\sigma_A = J\mathsf{S} \times Nx\sigma_A. \tag{2.2}$$

Here, $J\mathsf{S}$ is the number of projectiles per unit time; hence, $Nx\sigma_A$ is the mean number of events per projectile. If the target is thin enough so that $Nx\sigma_A \ll 1$, that number becomes identical with the probability P_A for a projectile to undergo an event A while interacting with the stopping medium, i.e.,

$$\mathsf{P}_A = Nx\sigma_A \qquad \text{for} \qquad Nx\sigma_A \ll 1. \tag{2.3}$$

Thus, cross sections are measured most conveniently with gas targets or thin foils where either N or x is small, respectively.

Eqs. (2.1–2.3) are roughly equivalent, and each of them serves an important purpose. Eq. (2.1) is the most basic one, dealing with one target particle only; it will be employed in theoretical determinations of cross sections from the equations of motion. Eq. (2.2) is most closely related to measurable quantities and is therefore utilized when cross sections are determined experimentally. Eq. (2.3) applies to probability statements about what happens to a projectile during passage through some small path element x; it serves as the starting point of penetration theory.

We shall encounter situations where (2.2) and (2.3) are not valid: It has been assumed in the step from from (2.1) to (2.2) that a scattering event is not influenced by the presence of other target particles. That assumption need not be fulfilled.

There is one major difference between the conventional macroscopic concept of a cross section and the present, statistical one. When you fire a bullet at some macroscopic target you will usually hit it if you have aimed at the right area and you won't if you have not. This is not so in the microscopic world governed by quantum effects. When defining a microscopic cross section as above you may be dealing with a product of some geometric cross section σ_{g} and a probability p_A,

$$\sigma_A = \sigma_{\mathrm{g}} \times \mathsf{p}_A. \tag{2.4}$$

The problem with (2.4) is that it may be hard to obtain independent information on σ_{g} and p_A. All you obtain from (2.2) is the product of the two quantities, and σ_{g} may not even be defined. If you have an idea about the magnitude of σ_{g}, you may, however, determine p_A from (2.4), and that way you get some understanding of whether or not σ_A corresponds to a well-defined area within which the projectile has to aim in order to initiate an event A with a reasonable degree of certainty.

There is a wide range of penetration phenomena where we do not need independent information on either σ_{g} or p_A. In cases where such information

is important, a more precise separation of the geometric factor than in (2.4) needs to be made. This point will come up in particular in Chapter 8.

2.2.2 Multiple Collisions; Poisson's Formula

In the preceding paragraph the probability for a collision event during a passage was assumed to be small. In penetration phenomena we deal most often with projectiles undergoing many collisions in an individual passage. Therefore we need some statistical information on the number of events in case P_A as given by (2.3) is not small.

Let us illustrate the situation geometrically (Fig. 2.2) by associating a 'black area' σ_A to each target particle. The number of events A is equal to the number of times a projectile hits such a black area. Then, (2.3) can be written in the form

$$\mathsf{P}_A = \frac{N\mathsf{S}x \times \sigma_A}{\mathsf{S}} = \frac{\text{total black area}}{\text{total area}} \tag{2.5}$$

provided that $\mathsf{P}_A \ll 1$ and that the target particles do not shadow each other systematically as, e.g., in a crystal. If the number of target particles $N\mathsf{S}x$ increases, e.g., due to increasing thickness x at constant number density N, the total black area will increase to the point where individual black areas overlap appreciably; ultimately, for $Nx\sigma_A \gg 1$, the entire area appears black. This implies that the probability for a projectile to undergo at least one event A is essentially equal to 1, but the actual number of events may be substantially larger.

Let us ask for the probability P_n for the projectile to initiate precisely n events A during its passage through the medium. In our geometrical picture this is the same as asking for the probability for n individual black areas to overlap with the trajectory of a given beam particle. Alternatively, we may associate a cylindrical volume

$$\mathsf{v} = x\sigma_A \tag{2.6}$$

with each trajectory and try to find the probability for n target particles to be located within one such volume. The latter question is a standard problem in kinetic gas theory: Given an ideal gas of average density N, what is the probability to find precisely n gas molecules within some specified volume v at any instant of time? The answer is given by the Poisson distribution,

$$\mathsf{P}_n = \frac{(N\mathsf{v})^n}{n!}\,\mathrm{e}^{-N\mathsf{v}}. \quad n = 0, 1, 2 \ldots \tag{2.7}$$

If you are unfamiliar with Poisson's formula you may wish to consult Appendix A.2.1 for an elementary derivation. The main assumptions entering into (2.7) are the following:

– the positions of any two or more gas molecules are uncorrelated, and
– the sample volume v must be small compared with the total volume filled with gas.

The latter assumption allows to consider the number of available atoms as practically unlimited; then one easily verifies the relationships:

$$\sum_{n=0}^{\infty} \mathsf{P}_n = 1 \tag{2.8}$$

and

$$\sum_{n=0}^{\infty} n\mathsf{P}_n = \langle n \rangle = N\mathsf{v}, \tag{2.9}$$

the brackets indicating an average. For the variance one finds[1]

$$\overline{(n - \langle n \rangle)^2} = \langle n \rangle. \tag{2.10}$$

Eq. (2.10) is a central property of the Poisson distribution. It implies that the relative fluctuation

$$\frac{\overline{(n - \langle n \rangle)^2}}{\langle n \rangle^2} = \frac{1}{\langle n \rangle} \tag{2.11}$$

goes to zero in the limit of large $\langle n \rangle$.

Let us now go back to the statistics of collision events. In order that (2.7) be applicable we must require that the positions of target particles be uncorrelated, i.e., that target particles act as if they were the constituents of an ideal gas. This may be an essential restriction; we shall come back to this point in Chapter 8. The requirement that v be small compared with the size of the container implies that $\sigma_A \ll \mathsf{S}$, cf. (2.6); this is generously satisfied in case of a macroscopic area S.

By combining (2.6) with (2.9) we find the average number of events A to be given by

$$\langle n \rangle = Nx\sigma_A \tag{2.12}$$

and, from (2.10), the fluctuation

$$\overline{(n - \langle n \rangle)^2} = \langle n \rangle = Nx\sigma_A. \tag{2.13}$$

Eq. (2.12) generalizes (2.2) to the case where $\langle n \rangle$ is not small. As an additional benefit we also have found an expression for the fluctuation in the number of events, (2.13).

[1] Notations $< \cdots >$ or $\overline{\cdots}$ are utilized synonymously to indicate averages, dependent on readability.

The probability P_0 for no event at all follows from (2.7) and (2.12) for $n = 0$,

$$\mathsf{P}_0 = \mathrm{e}^{-Nx\sigma_A}. \tag{2.14}$$

This is called Lambert & Beer's law and governs absorption phenomena.

In case of $Nx\sigma_A \ll 1$ we find that

$$\mathsf{P}_n \simeq \begin{cases} 1 - Nx\sigma_A & \text{for } n = 0 \\ Nx\sigma_A & \text{for } n = 1 \\ 0 & \text{for } n \geq 2 \end{cases} \tag{2.15}$$

up to first order in $Nx\sigma_A$. Thus (2.7) goes over into (2.3) in the limit where the probability for double events is vanishingly small, cf. (A.19) and (A.20) in Appendix A.2.1.

The Poisson distribution is discussed in mathematical terms in standard texts on probability theory (Feller, 1968). Its significance to kinetic gas theory was pointed out by v. Smoluchowski (1904), and the connection to penetration theory was drawn by Bohr (1915).

2.2.3 Energy Loss

Consider now specifically the process of energy loss by a charged particle moving through a stopping medium; in order to be sure that the collision events be distributed according to Poisson's formula, assume the medium to be a gas for the time being.

On account of the conclusions drawn from Fig. 1.1, ignore initially all angular scattering of the projectile. In colliding with the atoms or molecules of the gas a projectile may transfer part of its kinetic energy to those atoms and thus suffer a decrease in velocity. The observation of nearly equal track lengths (Fig. 1.1) indicates that the typical energy lost in a single encounter is small compared with the projectile energy.

Assume that the projectile can lose energy in discrete bits of T_j, with $j = 1, 2 \ldots$, and that $T_j \ll E$ for all j, where E is the projectile energy. T_j might represent the excitation levels above the ground state of a target atom or molecule.

While penetrating a layer of thickness Δx which is assumed small compared with the total penetration depth, a projectile loses an amount of energy ΔE given by

$$\Delta E = \sum_j n_j T_j, \tag{2.16}$$

where n_j is the number of collisions of type j, each leading to an energy transfer T_j.

In order to find the average energy loss $\langle \Delta E \rangle$ and its fluctuation for a great number of projectiles, let us employ the statistical arguments outlined in the

previous section with the one addition that we now deal with a spectrum of energy transfers T_j rather than one single possible event A.

For the average energy loss $\langle \Delta E \rangle$ we find from (2.16) that

$$\langle \Delta E \rangle = \sum_j \langle n_j \rangle T_j. \tag{2.17}$$

Introducing the *energy-loss cross section* σ_j for a quantum T_j according to (2.1) we find from (2.12)

$$\langle n_j \rangle = N \Delta x \, \sigma_j \tag{2.18}$$

and hence,

$$\langle \Delta E \rangle = N \Delta x \sum_j T_j \sigma_j. \tag{2.19}$$

Here,

$$S = \sum_j T_j \sigma_j \tag{2.20}$$

is the *stopping cross section*, and the ratio

$$\frac{\langle \Delta E \rangle}{\Delta x} = NS = N \sum_j T_j \sigma_j \tag{2.21}$$

is called the *stopping force* or *stopping power*[2]. While the stopping force is a property of the stopping medium, the stopping cross section is a microscopic quantity. In the literature one frequently finds the symbol S used for the stopping force rather than the stopping cross section. This should cause little confusion since the former has the dimension of [energy/length] while the latter is an [energy×area].

As defined by (2.21) the stopping force is a positive quantity. This is not a universal convention in the literature but reasonable to the extent that energy *loss* rather than *gain* is in focus. However, the function $\mathrm{d}E/\mathrm{d}x$ to be introduced below in (2.34) must be taken negative whenever the projectile energy decreases with time or pathlength.

2.2.4 Energy-Loss Straggling

Consider now the mean-square fluctuation Ω^2 in energy loss ΔE. According to (2.16) and (2.17) we have

[2] Evidently, the term 'stopping force' is in agreement with common nomenclature, while 'stopping power' would be the correct term for the energy loss per unit time. Nevertheless, the latter term has been in use for almost a century and is only slowly disappearing from the literature. Cf. Sigmund (2000).

$$\Delta E - \langle \Delta E \rangle = \sum_j (n_j - \langle n_j \rangle) T_j \tag{2.22}$$

and therefore

$$\Omega^2 = \overline{(\Delta E - \langle \Delta E \rangle)^2} = \sum_{j,l} \overline{(n_j - \langle n_j \rangle)(n_l - \langle n_l \rangle)} T_j T_l; \tag{2.23}$$

Now take the terms $j = l$ and $j \neq l$ separately. For $j = l$,

$$\overline{(n_j - \langle n_j \rangle)^2} = \langle n_j \rangle = N \Delta x \sigma_j \tag{2.24}$$

when the Poisson relation (2.13) applies and (2.18) is inserted. For $j \neq l$, split the average of the product into the product of averages

$$\overline{(n_j - \langle n_j \rangle)(n_l - \langle n_l \rangle)} = \overline{n_j - \langle n_j \rangle} \times \overline{n_l - \langle n_l \rangle} \tag{2.25}$$

because of the statistical independence of different types of collision events; since $\overline{n_j - \langle n_j \rangle} = 0$, drop all terms with $j \neq l$ in (2.23) and find

$$\Omega^2 = \sum_j \langle n_j \rangle T_j^2 = N \Delta x \sum_j T_j^2 \sigma_j. \tag{2.26}$$

In analogy with the stopping cross section, introduce the *straggling parameter*

$$W = \sum_j T_j^2 \sigma_j, \tag{2.27}$$

which has the dimension of [energy^2×area]. Just as the stopping cross section it is a microscopic property.

A word of caution is indicated with respect to the validity of the relations (2.19) and (2.26). Although these expressions are formally similar, (2.19) is much more general than (2.26). Little can go wrong with the derivation of (2.19); we shall see later that the stopping force is to some extent independent of the structure of the stopping medium. Conversely, not only was explicit use made of the Poisson relationship (2.13) in the derivation of (2.26), but also were collisions leading to different energy transfers T_j and T_l assumed statistically independent. The latter assumption is readily justified in a dilute stopping medium provided that the ion has no memory, i.e., does not undergo changes in state that may influence the stopping cross section. On the other hand, if the medium were closely packed like a solid or a liquid, there would be a more or less pronounced anticorrelation between collisions leading to different energy transfers; such effects will be analyzed in Chapter 8 and it will be found that straggling is sensitive to the structure of the stopping medium.

2.2.5 Differential Cross Section

Let us finally go over to the case of a continuous spectrum of energy loss in individual encounters; such a spectrum applies, e.g., to ionizing collisions with an atom, collisions with a molecule leading to dissociation, etc. You may then apply the present description in a heuristic sense, i.e., make the replacement

$$\sigma_j \to \frac{\mathrm{d}\sigma}{\mathrm{d}T}\,\Delta T_j \tag{2.28}$$

and let the interval size ΔT_j be sufficiently small to replace the sums in (2.20) and (2.27) by integrals. In short-hand notation this yields

$$S = \int T \mathrm{d}\sigma, \tag{2.29}$$

$$W = \int T^2 \mathrm{d}\sigma, \tag{2.30}$$

where

$$\mathrm{d}\sigma = \frac{\mathrm{d}\sigma(T)}{\mathrm{d}T}\,\mathrm{d}T \tag{2.31}$$

is called the *differential energy-loss cross section* and the integrations extend over the spectrum of possible energy transfers. According to (2.3) the quantity

$$\mathrm{d}\mathsf{P} = Nx\mathrm{d}\sigma \tag{2.32}$$

is the probability for a projectile to undergo a collision with energy loss[3] $(T, \mathrm{d}T)$ when interacting with the stopping medium under single-collision conditions, i.e., sufficiently small N and/or x.

2.2.6 Range

Up till now the layer thickness was assumed small compared with the penetration depth of the projectile. This made it possible to assume the projectile energy E to be essentially constant. In general the differential cross section and hence the microscopic parameters S and W will depend on energy. This energy dependence is essential for the understanding of the stopping of a projectile down to zero energy.

Consider first the case where the fluctuation in energy loss is negligibly small, as appears to be the case in Fig. 1.1. This implies that the projectile energy is a well-defined function of the penetration depth x,

[3] The symbol $(T, \mathrm{d}T)$ indicates the interval limited by T and $T + \mathrm{d}T$. Similarly, $(\mathbf{\Omega}, \mathrm{d}^2\mathbf{\Omega})$ indicates a solid angle $\mathrm{d}^2\mathbf{\Omega}$ around the unit vector $\mathbf{\Omega}$, and $(\mathbf{r}, \mathrm{d}^3\mathbf{r})$ indicates a volume element $\mathrm{d}^3\mathbf{r} = \mathrm{d}x\mathrm{d}y\mathrm{d}z$ located at a vector distance $\mathbf{r}$ from the origin.

$$E = E(x) \tag{2.33}$$

which obeys the differential equation

$$\frac{\mathrm{d}E}{\mathrm{d}x} = -NS(E) \tag{2.34}$$

that follows from (2.21). The minus sign accounts for the decrease in projectile energy. Equation (2.34) has the solution

$$x = \int_{E(x)}^{E_0} \frac{\mathrm{d}E'}{NS(E')} \tag{2.35}$$

in implicit form, where $E_0 = E(0)$ is the initial energy. In particular, the total path length or range R is found by setting $E(x) = 0$, i.e.,

$$R = \int_0^{E_0} \frac{\mathrm{d}E'}{NS(E')}. \tag{2.36}$$

This estimate of the range, based on the *continuous-slowing-down-approximation* (csda) (2.34), is valid only in the case of negligible straggling; (2.36) is not strictly identical with the average range when statistical fluctuations become significant.

An estimate of the fluctuation Ω_R^2 in range – valid for small Ω_R^2 – can be found as follows. When slowing down from E to some energy $E - \Delta E$, the projectile travels a path length $\Delta x \simeq \Delta E/NS(E)$ on the average; the corresponding fluctuation is of the order of $\Omega_x^2 \simeq \Omega^2/(\mathrm{d}E/\mathrm{d}x)^2$; this follows most easily by dimensional arguments. Insertion of Ω^2 from (2.26) and (2.27) as well as (2.34) and Ω_x yields

$$\Omega_x^2 \simeq \frac{NW(E)\Delta E}{\big[NS(E)\big]^3} \tag{2.37}$$

for the *fluctuation in projectile path length* during slowing down from E to $E - \Delta E$. Consequently, the *fluctuation in total range* Ω_R^2 is found by integration down to zero energy,

$$\Omega_R^2 \simeq \int_0^{E_0} \mathrm{d}E' \frac{NW(E')}{\big[NS(E')\big]^3}. \tag{2.38}$$

If a precise meaning is to be assigned to (2.38) some detailed information on the shape of the statistical distributions of energy loss and range is needed. This point will be considered in Chapter 8 and Volume II.

There is little in the substance of the present section that cannot be found in the review by Bohr (1948). Historically, the most important step was the experience that alpha and beta rays, unlike gamma rays, lose energy gradually rather than getting absorbed. That observation appears to date

back to Sklodowska-Curie (1900), while the notion of stopping power may be found with Bragg and Kleeman (1905). At the same time and independently, Leithäuser (1904) demonstrated that cathode rays lose energy in penetrating thin metal foils. The first attempt to relate the stopping force to an atomic stopping cross section dates back to Thomson (1912). Extensive range calculations were made by Darwin (1912). The treatment of fluctuations in energy loss and range dates back to Bohr (1915).

2.3 Electronic and Nuclear Stopping

2.3.1 General Considerations

The present section serves as a first qualitative orientation on the dominating mechanisms of energy loss. This problem will have to be treated again and again as we dig deeper into the field.

Let us keep to the case of a charged particle penetrating through a gaseous stopping medium. At moderate velocities a projectile may experience a change in speed in a collision with an individual gas atom or molecule by means of the following processes:

- excitation or ionization of target particles,
- transfer of energy to center-of-mass motion of target atoms,
- changes in the internal state of the projectile, and
- emission of radiation.

In a rough manner the first process may be characterized as a loss of projectile energy into kinetic and potential energy of target electrons while the second process deals essentially with energy transfer to target nuclei; note that the mass, and therefore the kinetic energy of target atoms or molecules, is essentially contained in the nuclei. Therefore the first process is usually called 'electronic energy loss' and the second 'nuclear energy loss'. One may also refer to electronic energy loss as the transfer of internal energy to the target particle as opposed to nuclear energy loss as the transfer of center-of-mass energy. Therefore one may find the notions of *inelastic* and *elastic* energy loss, although the reader may be inclined to assign a different meaning to those concepts, depending on background. Those familiar with neutron or photon scattering may call a scattering event elastic if the incident particle does not suffer energy loss; the present notion of elastic collisions implies only that *energy is not transferred into internal degrees of freedom of the target or projectile*. Moreover, one may be inclined to call a collision event inelastic whenever it is not elastic, and consequently split the collision *cross section* into an elastic and an inelastic contribution. That is certainly a most reasonable concept. Nevertheless, in the stopping literature, many authors tend to split the *energy loss in an individual event* into an elastic and an inelastic contribution, thereby calling the nuclear energy loss elastic and the

electronic one inelastic, but it may take some time to realize that this is what those authors do. In order to minimize confusion I shall avoid the notion of an inelastic collision as much as possible and most often talk about nuclear and electronic energy loss or stopping.

Coming back to the above classification of energy-loss processes, ignore changes in the projectile state for the time being. The estimates put forward presently refer to a penetrating point charge. Emission of radiation, especially bremsstrahlung, is a rather different process which becomes important at projectile speeds approaching the velocity of light.

In principle, various processes at the nuclear or subnuclear level would have to be incorporated into the above classification scheme. Whether or not this is important does not only depend on the velocity range and the projectile-target combination in question but also on the reader's motivation to study penetration phenomena: If the interest is in nuclear or high-energy physics, this book may be consulted for information on atomic phenomena that influence penetration properties important in the analysis of nuclear or high-energy processes. If, on the other hand, the interest is in atomic, solid-state, or biological phenomena, nuclear processes may have to be included as an energy sink (or source) if important, along with all other pertinent effects. Initially we shall concentrate on electronic and nuclear energy loss.

In case of doubt, you may do well by defining energy loss of a charged particle as the loss in *kinetic energy of its center-of-mass* in the laboratory frame of reference. For an ion carrying electrons, you may, alternatively, operate with *the loss of kinetic energy of the nucleus*. The difference between the two definitions is less than 0.1 %, i.e., below the accuracy of available experimental techniques.

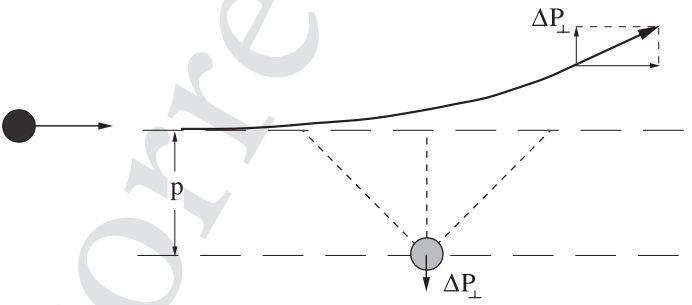

Fig. 2.3. A 'soft' scattering event with momentum transfer $P_\perp$ perpendicular to the beam direction

2.3.2 Momentum and Energy Transfer in Free-Coulomb Collision

For a first qualitative orientation, oversimplify a gaseous stopping medium and treat it as an ideal-gas mixture of free nuclei and electrons. The elementary

collision event is, then, the interaction of the projectile, i.e., a point charge e_1 with mass m_1 moving with velocity v, with a target particle of mass m_2 and charge e_2; the target particle can be either a nucleus or an electron. m_2 will turn into a capital M_2 for a nucleon and into m for an electron.

In accordance with Fig. 1.1 on page 4, ignore events leading to a substantial change in projectile velocity; the projectile will be considered to cause an external force that imparts momentum to a target particle that is initially at rest. The collision event is sketched in Fig. 2.3. If the target particle receives only a small momentum it can be considered stationary for the duration of the collision and the momentum transfer is given by

$$\Delta\mathbf{P} = \int_{-\infty}^{\infty} \mathrm{d}t\, \mathbf{F}(t), \tag{2.39}$$

where $\mathbf{F}(t)$ is the Coulomb force[4]

$$F(t) = \frac{e_1 e_2}{p^2 + (vt)^2} \tag{2.40}$$

between the two point charges as a function of time t. Splitting the force into components parallel and normal to the projectile velocity $\mathbf{v}$ (Figure 2.4) we find

$$\Delta P_{\parallel} = e_1 e_2 \int_{-\infty}^{\infty} \mathrm{d}t\, \frac{vt}{(p^2 + v^2 t^2)^{3/2}} = 0 \tag{2.41}$$

and

$$\Delta P_{\perp} = e_1 e_2 \int_{-\infty}^{\infty} \mathrm{d}t\, \frac{p}{(p^2 + v^2 t^2)^{3/2}} = \frac{2|e_1 e_2|}{pv}, \tag{2.42}$$

where p, the *impact parameter*, is the distance between the straight-line trajectory and the initial position of the target. It has been assumed for convenience that this distance is reached at time $t = 0$.

Equations (2.41) and (2.42) constitute a special case of the *momentum approximation* in classical scattering theory. It can be understood as the first term in a perturbation expansion in powers of the interaction between two particles[5]. Because of the symmetry of the Coulomb interaction the longitudinal momentum transfer $\Delta P_{\parallel}$ vanishes to first order, cf. (2.41). Hence momentum is only transferred normal to the projectile velocity in that approximation.

We may find an estimate for the effective collision time τ from the expression

$$\Delta P_{\perp} \simeq F_{\max}\, \tau \tag{2.43}$$

[4] From now on electromagnetic quantities will be taken in Gaussian units. Pertinent relationships have been collected in Appendix A.1.1.

[5] This expansion will be discussed in more detail in Appendix A.3.1.

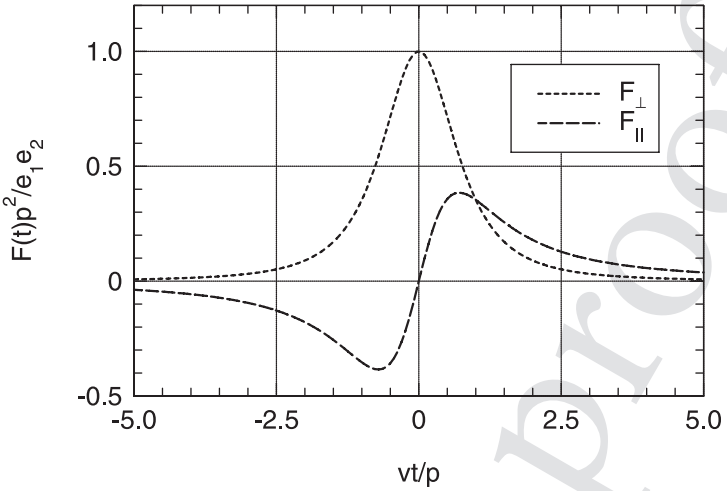

Fig. 2.4. Time dependence of the force parallel and perpendicular to the beam direction according to (2.41) and (2.42)

where $F_{\max}$ is the force at closest approach ($t = 0$) and directed normal to the initial velocity. With $F_{\max} = |e_1 e_2|/p^2$ and by comparison to (2.42) one finds

$$\tau \simeq \frac{2p}{v}, \tag{2.44}$$

i.e., the two particles interact effectively over a length $\simeq 2p$ of the incoming trajectory. This has been indicated by the stipled lines in Fig. 2.3. Note that the Coulomb force has half its maximum value at a distance $p\sqrt{2}$.

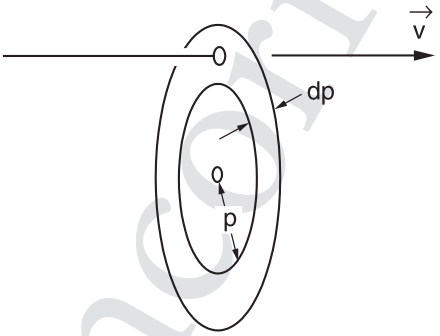

Fig. 2.5. Differential cross section and impact parameter

From (2.42) follows

$$T = \frac{\Delta P_\perp^2}{2m_2} \simeq \frac{2e_1^2 e_2^2}{m_2 v^2 p^2} \tag{2.45}$$

for the energy T lost to particle 2 as a function of impact parameter p. In order that such a collision lead to an energy transfer in an interval $(T, \mathrm{d}T)$, the projectile must aim at a cross-sectional area

$$\mathrm{d}\sigma = 2\pi p \mathrm{d}p = |\frac{\mathrm{d}(\pi p^2)}{\mathrm{d}T}|\mathrm{d}T \tag{2.46}$$

around the target (Fig. 2.5). By differentiation of (2.45) one finds

$$\mathrm{d}\sigma \simeq 2\pi \frac{e_1^2 e_2^2}{m_2 v^2} \frac{\mathrm{d}T}{T^2}. \tag{2.47}$$

Eq. (2.47) is more accurate than (2.45) from which it was derived. In fact it is an exact version of Rutherford's cross section for Coulomb scattering except for the fact that no upper limit for T is specified by (2.45). A more rigorous derivation of Rutherford's law for classical nonrelativistic scattering will be given in Chapter 3; at present, remember that for a head-on collision ($p = 0$) between a projectile of initial velocity v and a target of initial velocity zero, the conservation laws of energy and momentum, applied to one-dimensional motion, require the final velocity of the target to be

$$v_{\max} = \frac{2m_1}{m_1 + m_2} v. \tag{2.48}$$

This yields a maximum energy transfer

$$T_{\max} = m_2 v_{\max}^2/2 = \gamma E \tag{2.49}$$

with

$$\gamma = \frac{4m_1 m_2}{(m_1 + m_2)^2}, \tag{2.50}$$

where $E = m_1 v^2/2$.

2.3.3 Stopping and Straggling: Preliminary Estimates

When (2.47) is inserted into (2.29) and (2.30) on p. 36 one finds

$$S \simeq 2\pi \frac{e_1^2 e_2^2}{m_2 v^2} \ln \frac{T_{\max}}{T_{\min}}; \tag{2.51}$$

$$W \simeq 2\pi \frac{e_1^2 e_2^2}{m_2 v^2} (T_{\max} - T_{\min}). \tag{2.52}$$

A lower integration limit corresponding to a truncation of the interaction (2.45) at large impact parameters p was introduced in order to remove an apparent divergence from the stopping cross section. Ways of specifying such a cutoff will be discussed in sections 2.3.4 and 2.3.7.

Let us first consider a situation where all energy loss to electrons is ignored. Take N to be the number density of nuclei of charge $e_2 = Z_2 e$ and mass $m_2 = M_2$. e is the elementary charge and Z_2 the atomic number. Then, according to (2.19) and (2.26),

$$\langle \Delta E \rangle_{\mathrm{n}} \simeq N \Delta x \times \frac{4\pi e_1^2 Z_2^2 e^2}{M_2 v^2} L_{\mathrm{n}}, \tag{2.53}$$

$$\langle (\Delta E - \langle \Delta E \rangle)^2 \rangle_{\mathrm{n}} \simeq N \Delta x \times \frac{4\pi e_1^2 Z_2^2 e^2 m_1^2}{(m_1 + M_2)^2}, \tag{2.54}$$

where the subscript 'n' indicates nuclear energy loss. In (2.53), the abbreviation

$$L_{\mathrm{n}} = \frac{1}{2} \ln \left(\frac{T_{\max}}{T_{\min}} \right)_{\mathrm{n}} \tag{2.55}$$

has been introduced while in (2.54), $T_{\min}$ has been dropped.

Next, consider the opposite case where all energy loss to nuclei is ignored. With a number density NZ_2 of electrons (mass m, charge $-e$) one finds correspondingly

$$\langle \Delta E \rangle_{\mathrm{e}} \simeq N \Delta x \times \frac{4\pi e_1^2 e^2 Z_2}{m v^2} L_{\mathrm{e}}, \tag{2.56}$$

$$\langle (\Delta E - \langle \Delta E \rangle)^2 \rangle_{\mathrm{e}} \simeq N \Delta x \times \frac{4\pi e_1^2 e^2 Z_2 m_1^2}{(m_1 + m)^2}, \tag{2.57}$$

where the subscript 'e' indicates electronic energy loss.

Finally, take the ratios of equivalent quantities for nuclear and electronic stopping,

$$\frac{\langle \Delta E \rangle_{\mathrm{n}}}{\langle \Delta E \rangle_{\mathrm{e}}} \simeq \frac{m}{M_2} Z_2 \frac{L_{\mathrm{n}}}{L_{\mathrm{e}}}, \tag{2.58}$$

$$\frac{\langle (\Delta E - \langle \Delta E \rangle)^2 \rangle_{\mathrm{n}}}{\langle (\Delta E - \langle \Delta E \rangle)^2 \rangle_{\mathrm{e}}} \simeq \left(\frac{m_1 + m}{m_1 + M_2} \right)^2 Z_2. \tag{2.59}$$

The ratio of the mean energy losses, (2.58), is obviously dominated by the factor mZ_2/M_2 which is less than 10^{-3}. Regardless of the accurate values of $T_{\max}$ and $T_{\min}$ the ratio of logarithms will not compensate for this large

difference unless L_e is close to zero. That case will show up only at low projectile velocities where target electrons cannot be considered free.

Thus, under the present somewhat oversimplified assumptions, the *mean energy loss* is heavily dominated by the electronic contribution for both light and heavy point charges, despite the fact that the *maximum energy transfer* from a heavy projectile to a nucleus is many times larger than that to an electron. In order to appreciate the physical origin of this very central conclusion, note that the mean energy loss receives a substantial contribution from rather gentle collisions of the type sketched in Fig. 2.3 on page 39. While the average *momentum* transferred to target electrons does not differ dramatically from the average momentum transferred to target nuclei because forces are comparable, a pronounced difference occurs in transferred *energy*, cf. (2.45), where the mass enters into the denominator.

Next, consider the ratio of fluctuations, (2.59). If the projectile is an electron ($m_1 = m$), that ratio becomes $4Z_2(m/M_2)^2$ which is $\sim 10^{-7}$ or less. Thus, electronic processes dominate even more strongly than in case of the mean energy loss. For a heavy projectile on the other hand, $m_1 = M_1$, the ratio is less than 1 for $M_1 \ll M_2$ but may exceed 1 for $M_1 \geq M_2$.

The physical reason for the significance of nuclear energy losses in straggling is to be found in the high-energy-loss tail of the Rutherford spectrum (2.47). Evidently that tail is more important in the integral $\int T^2 \mathrm{d}\sigma$ than in $\int T \mathrm{d}\sigma$. The presence of this tail makes it a rather delicate task to estimate the actual shape of an energy loss profile. Substantial effort will be devoted to this task in Chapter 9.

The dominating role of the electronic stopping force in the penetration of alpha and beta rays was recognized in the earliest investigations into the field and became the basis of Thomson's stopping model where stopping and ionization were treated essentially synonymously (Thomson, 1912). With regard to stopping force and straggling, the present discussion does not go beyond what can be found in the monographs by Bohr (1948) and especially Bonderup (1981).

2.3.4 Adiabatic Limit to Electronic Stopping

According to (2.58) the stopping force on a point charge is essentially electronic. From (2.56) we obtain the electronic stopping cross section

$$S_e = \frac{4\pi Z_2 e_1^2 e^2}{mv^2} L_e \tag{2.60}$$

where $L_e = \frac{1}{2}\ln(T_{max}/T_{min})_e$. A quantity L defined by (2.60) is called a *stopping number*. Consequently, L_e denotes the *electronic stopping number*. For a heavy projectile, $m_1 \gg m$, (2.49) and (2.50) yield

$$(T_{max})_e = 2mv^2. \tag{2.61}$$

In this section an estimate of the lower limit $T_{\min}$ of energy transfer will be derived.

Note first that $T_{\min}$ is strictly zero in the case of a free, isolated target electron. Thus, the long-range Coulomb interaction causes a logarithmic divergence of the stopping cross section. There are two most obvious ways of removing this artifact, taking into account the *binding* of electrons to the atoms or molecules in a neutral stopping medium, or to consider *screening* of the Coulomb interaction. Let us consider binding here.

Offhand one might be inclined to incorporate electronic binding forces by merely inserting the lowest electronic excitation energy of a target atom or molecule for $(T_{\min})_{\mathrm{e}}$ or, as suggested by Thomson (1912), the lowest ionization energy. While this is justified for a qualitative estimate, it turned out that the argument of Bohr (1913, 1915), based on the simple picture of a spring force between electron and nucleus does not only lead to a different quantitative result but also has a very close quantal analog.

Bohr treated the individual target electron as a classical harmonic oscillator with a resonance angular frequency of, say, ω_0. When an external force F acts on such an oscillator during a limited period of time τ, the exchange of momentum depends essentially on the magnitude of τ compared with the oscillation period $2\pi/\omega_0$. For $\tau \ll 2\pi/\omega_0$, the oscillator takes up an impulse $\sim F \times \tau$ just as if it were a free particle; this effect may be experienced by giving a push with a hammer to the steel ball of a pendulum. Conversely, for $\tau \gg 2\pi/\omega_0$, the oscillator tends to respond adiabatically to the external force and it will tend to calm down as the disturbance vanishes even in the absence of damping forces. Thus, the takeup of momentum will be much smaller than that experienced by an otherwise equivalent free particle.

The duration of the force acting on a target electron from a moving projectile is given approximately by (2.44) for a soft collision; hence an effective adiabatic cutoff occurs at an impact parameter where $2p/v \ll 2\pi/\omega_0$, i.e., $p_{\max}$ will be of the order of

$$p_{\max} \sim \frac{v}{\omega_0} \tag{2.62}$$

apart from a numerical constant that has to be determined by a more accurate calculation. Eq. (2.62) specifies *Bohr's adiabatic radius.*

Combining (2.62) with (2.45) we obtain[6]

$$T_{\min} \sim \frac{2e_1^2 e^2 \omega_0^2}{mv^4} \tag{2.63}$$

or

$$L = \frac{1}{2} \ln \frac{T_{\max}}{T_{\min}} = \ln \frac{Cmv^3}{|e_1 e| \omega_0} \tag{2.64}$$

[6] The subscript 'e' will be dropped when there is no doubt that we deal with electronic stopping.

with a yet undetermined constant C which is ~ 1 but will be evaluated in Sect. 4.5.1.

2.3.5 Relativistic Extension

While relativistic effects play a role in particle penetration on all levels, most of the phenomena discussed in this book are observable equally well at non-relativistic and relativistic velocities. Hence, relativity may affect quantitative details but – with very few exceptions – is not the essential aspect. Therefore the strategy will be followed to present nonrelativistic treatments and add pertinent relativistic corrections where appropriate.

The present section serves the purpose to extend the simple treatment of Coulomb scattering discussed in Sect. 2.3.2 to relativistic velocities. Appendix A.3.2 recapitulates pertinent formulas from special relativity.

On the basis of the Lorentz transformation for electromagnetic fields (cf. Appendix A.3.2) one finds the following relativistic extensions of (2.41) and (2.42)[7],

$$\Delta P_{\parallel} = e_1 e_2 \int_{-\infty}^{\infty} \mathrm{d}t \, \frac{\gamma_v v t}{(p^2 + (\gamma_v v t)^2)^{3/2}} = 0 \tag{2.65}$$

and

$$\Delta P_{\perp} = e_1 e_2 \int_{-\infty}^{\infty} \mathrm{d}t \, \frac{\gamma_v p}{(p^2 + (\gamma_v v t)^2)^{3/2}} = \frac{2|e_1 e_2|}{pv}, \tag{2.66}$$

where

$$\gamma_v = \frac{1}{\sqrt{1 - v^2/c^2}}. \tag{2.67}$$

It is seen that there is no change in the momentum transfer at a given impact parameter, even though the maximum force has been enhanced by a factor γ_v. This implies that the collision time in (2.43) has become smaller by the same factor, i.e.,

$$\tau \simeq \frac{2p}{\gamma_v v} \tag{2.68}$$

instead of (2.44). This leads to a change in the adiabatic radius (2.62)

$$p_{\max} \sim \frac{\gamma_v v}{\omega_0} \tag{2.69}$$

[7] An attempt has been made to use a notation that should prevent the reader from mixing up the symbol γ_v in (2.65 – 2.67) with the quantity γ defined in eq. (2.50).

which in turn affects the minimum energy transfer (2.63) in an electronic collision,

$$T_{\min} \sim \frac{2e_1^2 e^2 \omega_0^2}{m\gamma_v^2 v^4}. \tag{2.70}$$

In order to find the maximum energy transfer in a binary collision between a heavy particle and an electron, look at a central collision in a reference frame in which the projectile is at rest. Here the electron moves with a velocity $-\boldsymbol{v}$ before and $\boldsymbol{v}$ after the collision. This implies a momentum $\boldsymbol{P'} = m\gamma_v \boldsymbol{v}$ and a total energy $E'_{\text{tot}} = m\gamma_v c^2$. Lorentz transformation into the laboratory system yields the energy in the laboratory frame,

$$E_{\text{tot}} = \gamma_v (E'_{\text{tot}} + vP') \tag{2.71}$$

and, hence, an energy transfer

$$T_{\max} = E_{\text{tot}} - mc^2 = 2m\gamma_v^2 v^2. \tag{2.72}$$

This results in a stopping number

$$L = \frac{1}{2} \ln \frac{T_{\max}}{T_{\min}} = \ln \frac{Cm\gamma_1^2 v^3}{|e_1 e|\omega_0} \tag{2.73}$$

instead of (2.64). It is a preliminary estimate which will be modified in Sect. 4.2.3.

2.3.6 Validity of Classical-Orbit Picture

So far, moving particles have been assigned classical orbits, and the limitations imposed by quantum mechanics were barely mentioned. The tacit justification of this procedure lies in the fact that we have been dealing with Coulomb interaction only; indeed, the differential cross section for scattering of two point charges on each other is known to be identical with Rutherford's law when calculated on the basis of nonrelativistic quantum mechanics (Gordon, 1928). This will be shown in Chapter 3. Hence, even though the actual state of motion will differ from classical Kepler orbits, the difference may be argued to be immaterial since the energy-loss spectrum in an individual collision event is unaffected by quantal corrections.

This simplifying feature need no longer be true

- when the force between the particles is not Coulomb-like,
- in the presence of binding forces, and
- at relativistic velocities.

Any of these three situations may occur in penetration phenomena. In addition we shall also need to consider spatial correlations in collision problems.

For all these reasons an estimate of the range of validity of the classical-orbit picture is needed.

From the point of view of penetration theory for swift charged particles it is most often the gentle collisions leading to small energy transfers that are considered most representative. Not only are those events by far the most frequent ones – as is seen from (2.47) – they also offer a number of challenges due to their long-range nature that suggests the possibility of collective effects in dense stopping media. Nevertheless close collisions, although rare, do occur and are not insignificant as is evidenced by the occurrence of $T_{\max}$ in the expressions for stopping force and straggling.

In the present context gentle collisions are considered mainly since we know already that binding corrections play a role in the determination of the lower limit $T_{\min}$ of the energy-loss spectrum in (2.60), and hence that the assumption of free-Coulomb scattering becomes invalid in that limit.

Go back once again to Fig. 2.5 on page 41. In order to estimate the limitations of a classical orbit we may try to find the lateral spreading of a wave packet centered around the straight projectile path depicted there.

According to Williams (1945) and Bohr (1948) the physical situation is as follows. One may try to pin down an impact parameter p with an uncertainty δp by constructing a Gaussian wave packet with a lateral spread δp, thereby introducing a transverse momentum δP_1 of the order of

$$\delta P_1 \sim \frac{\hbar}{2\delta p} \tag{2.74}$$

according to the Heisenberg uncertainty principle[8]. At the same time an uncertainty in the impact parameter results in an uncertainty in momentum transfer, δP_2 according to (2.42),

$$\delta P_2 \sim \delta p \left|\frac{\mathrm{d}(\Delta P_\perp)}{\mathrm{d}p}\right| = \frac{2|e_1 e_2|}{p^2 v} \times \delta p, \tag{2.75}$$

where $\Delta P_\perp$ follows from (2.42). The uncertainty principle implies that these two uncertainties are uncorrelated. We may estimate the total uncertainty from the sum of squares,

$$\delta P^2 \sim \delta P_1^2 + \delta P_2^2. \tag{2.76}$$

This quantity takes on its minimum value when δp^2 is chosen to be

$$\delta p^2_{\min} = \frac{\hbar p^2 v}{4|e_1 e_2|} \tag{2.77}$$

and $\delta P_{\min}$ becomes, then,

$$\delta P_{\min} \sim \sqrt{\frac{2|e_1 e_2|\hbar}{p^2 v}}. \tag{2.78}$$

[8] Appendix A.4.1 reviews Gaussian wave packets for the interested reader.

In order that the momentum transfer at a given impact parameter $p \pm \delta p_{\min}$ be well-defined we have to require that

$$\frac{\delta P_{\min}}{\Delta P_\perp} \sim \sqrt{\frac{\hbar v}{2|e_1 e_2|}} \ll 1 \tag{2.79}$$

In the notation of Bohr (1948) this reads

$$\kappa = \frac{2|e_1 e_2|}{\hbar v} \gg 1 \tag{2.80}$$

or

$$v \ll 2v_0 \left|\frac{e_1 e_2}{e^2}\right|, \tag{2.81}$$

where the Bohr velocity $v_0 = e^2/\hbar = c/137$ is the orbital speed of an electron in the ground state of a hydrogen atom, c being the speed of light in vacuum (Appendix A.1.2).

If the target particle is an electron, (2.81) reads

$$v \ll 2Z_1 v_0. \tag{2.82}$$

For low charge numbers Z_1 the limit imposed by (2.82) is rather severe. For alpha particles it lies at 1.6 MeV.

Now, the whole description of a projectile interacting with a target electron at rest can only be meaningful provided that

$$v \gg v_0, \tag{2.83}$$

i.e., if the projectile speed substantially exceeds some characteristic orbital velocity of the target electrons which has been set to be the Bohr velocity v_0. For low charge numbers, (2.82) is in direct conflict with (2.83). We may therefore conclude that the theory of electronic stopping for electrons and positrons is intrinsically quantal. Conversely, for heavier particles, and in particular for heavy ions with $e_1 \gg e$, (2.82) specifies a velocity range within which the assumptions underlying Bohr's classical stopping formula (2.64) are approximately valid.

2.3.7 Screening in Nuclear Stopping

There were good reasons to ignore nuclear stopping for a while. After all, electronic energy loss appears to dominate the stopping force on point charges by more than three orders of magnitude. This estimate, however, is based on the assumption that the nuclear stopping force does not diverge, i.e., that some mechanism is going to limit the Coulomb interaction between projectile and target nucleus to a finite range.

The keyword is *screening*. Indeed, if the stopping medium consists of neutral atoms or molecules, the Coulomb force between a point charge and a nucleus comes into action only when the point charge penetrates the electron shells. Thus, an effective maximum impact parameter $(p_{\max})_{\mathrm{n}}$ for nuclear collisions is equivalent to a representative radius a of the atomic or molecular electron cloud. Let us be satisfied for the moment with the statement that a is of the order of or less than the Bohr radius a_0 (cf. Appendix A.1.2).

Why don't we use Bohr's adiabaticity limit to find $(p_{\max})_{\mathrm{n}}$ as was done in electronic stopping? After all, nuclei are bound to each other in molecules and solids, approximately by oscillator forces. Well, in order that such an adiabatic limit be significant, it has to be smaller than a_0, or

$$v \leq a_0\omega = v_0\frac{\hbar\omega}{2\mathrm{R}} \tag{2.84}$$

according to (2.62), where ω is an effective binding frequency. Here, R is the Rydberg energy, R = 13.6 eV. (Appendix A.1.2). For typical vibrational frequencies of atoms in molecules, $\hbar\omega$ lies in the range around or below 0.1 eV; hence, nuclear collisions become adiabatic at projectile speeds that are at least two orders of magnitude lower than what we considered so far. Note that an alpha particle at a velocity $v = v_0$ carries a kinetic energy of about 100 keV (cf. problem 1.1 on page 22).

Incidentally, for nuclear stopping the condition for validity of the classical-orbit picture, (2.81) reads

$$v \ll 2Z_1Z_2v_0. \tag{2.85}$$

This is less stringent than (2.82) because of the occurrence of $Z_2 \geq 1$. We may conclude that nuclear collisions may follow the laws of classical mechanics over a considerably wider range of projectiles and speeds than what was found for electronic collisions.

Let us get back to screening and insert $(p_{\max})_{\mathrm{n}} = a$ into (2.45). This yields an effective minimum energy loss in nuclear collisions,

$$(T_{\min})_{\mathrm{n}} = \frac{2}{M_2v^2}\frac{e_1^2Z_2^2e^2}{a^2} \tag{2.86}$$

or

$$L_{\mathrm{n}} = \frac{1}{2}\ln\left(\frac{T_{\max}}{T_{\min}}\right)_{\mathrm{n}} \simeq \ln 2\varepsilon, \tag{2.87}$$

where

$$\varepsilon = \frac{M_2}{M_1+M_2}\frac{Ea}{e_1Z_2e} \tag{2.88}$$

and M_2 is the nuclear mass. ε is a dimensionless measure of the projectile energy that is of central significance in nuclear stopping (Lindhard et al., 1968).

2.4 Multiple Scattering

2.4.1 Small-Angle Approximation

Stopping and scattering are closely related phenomena in particle penetration. Strictly speaking you cannot deal with one and ignore the other. From a formal point of view it might look appealing to treat both phenomena at the same time, representing longitudinal and transverse changes in velocity, respectively. Yet the dominating processes will turn out to differ in the two cases. This discourages a joint treatment from a physical point of view. Instead one may come a long way by treating the change in projectile speed as independent of the changes in direction of motion.

Switch over to scattering and ignore all energy loss for a while. As in the case of stopping we normally deal with a sequence of events in particle penetration. Thus, the equivalent of stopping theory is the theory of *multiple scattering*. The formal treatment will largely turn out to be a generalization of the statistical theory of stopping into two dimensions.

Let us again take our starting point at the experimental fact demonstrated in Fig. 1.1 on page 4 that the trajectories of alpha particles are essentially straight lines. This means that small-angle scattering events appear to dominate.

One may at different stages ascribe different meanings to the notion of a 'small' angle. The term *small-angle approximation*, however, will consistently imply that the respective angle, say, θ, is small in an *absolute* sense so that the relations

$$\sin\theta \simeq \theta;\ \cos\theta \simeq 1 \tag{2.89}$$

hold within some prescribed accuracy.

Let us then have a look at the trajectory of an alpha particle, sketched schematically in Fig. 2.6. If all energy loss is ignored, the motion under a series of small-angle scattering events can be characterized by the projection on a plane perpendicular to the initial direction of motion. Introducing spherical polar coordinates v, α and χ and applying the small-angle approximation we find the expression

$$\begin{aligned}\mathbf{v} &= (v\cos\alpha, v\sin\alpha\cos\chi, v\sin\alpha\sin\chi)\\ &\approx v(1, \alpha\cos\chi, \alpha\sin\chi)\end{aligned} \tag{2.90}$$

for the velocity vector of the projectile if the initial direction of motion is directed along the x-axis. Thus, pertinent information on the direction of motion is contained in a two-dimensional vector $\boldsymbol{\alpha}$,

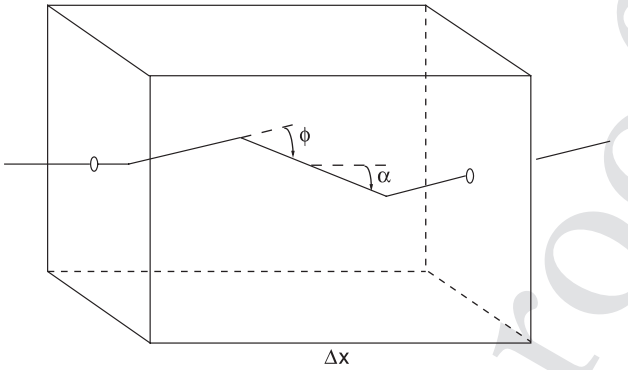

Fig. 2.6. Trajectory of an alpha particle during multiple scattering (schematically). α denotes the angle between the scattered particle and the initial beam direction and ϕ the scattering angle in an individual event

$$\boldsymbol{\alpha} = (\alpha \cos \chi, \alpha \sin \chi) \tag{2.91}$$

which represents the lateral component of a unit vector pointing in the instantaneous direction of motion of the projectile.

2.4.2 Statistics

Now let the projectile be able to undergo a discrete spectrum of scatterings at such vectorial angles $\boldsymbol{\phi}_j$, $j = 1, 2 \ldots$, and let the cross sections for these events be σ_j. If, during an individual passage, the projectile undergoes n_j deflections at angle $\boldsymbol{\phi}_j$, the final direction of motion is determined by the vector

$$\boldsymbol{\alpha} = \sum_j n_j \boldsymbol{\phi}_j \tag{2.92}$$

perpendicular to the initial velocity. This relation is a two-dimensional analog of (2.16). Consequently, averages can be found in the same way as in the treatment of energy loss.

In particular, the average deflection follows by analogy with (2.19),

$$\langle \boldsymbol{\alpha} \rangle = N \Delta x \sum_j \boldsymbol{\phi}_j \sigma_j. \tag{2.93}$$

This quantity will most often be zero, namely whenever the scattering centers look azimuthally symmetric to the projectile; then σ_j will be independent of the azimuth of the scattering angle $\boldsymbol{\phi}_j$, and the sum (or integral) (2.93) vanishes according to (2.91) since $\int_0^{2\pi} d\chi \cos \chi = \int_0^{2\pi} d\chi \sin \chi = 0$.

Next, the mean-square deflection angle follows by analogy to (2.23) and (2.26),

$$\overline{(\boldsymbol{\alpha} - \langle\boldsymbol{\alpha}\rangle)^2} = N\Delta x \sum_i \phi_i^2 \sigma_i = \langle\alpha^2\rangle, \tag{2.94}$$

and this quantity is nonzero if only one $\sigma_i \neq 0$. Here the first identity is general while the second implies azimuthal symmetry.

As in Sect. 2.2.3 we go over to continuum notation and write (2.94) in the form

$$\langle\alpha^2\rangle = N\Delta x \int \phi^2 \mathrm{d}\sigma \tag{2.95}$$

where $\mathrm{d}\sigma$ as given by

$$\mathrm{d}\sigma = K(\boldsymbol{\phi}) d^2\boldsymbol{\phi} \tag{2.96}$$

is the differential cross section for scattering into the solid angle $(\boldsymbol{\phi}, d^2\boldsymbol{\phi})$. In the considered case of azimuthal symmetry we have $K(\boldsymbol{\phi}) \equiv K(\phi)$, where ϕ is the polar scattering angle.

While the overall number of scattering events undergone by a projectile during a passage is typically a large number, the situation becomes different when attention is limited to large scattering angles. Indeed, take the probability

$$P(\alpha^*) = Nx \int_{\phi > \alpha^*} \mathrm{d}\sigma \tag{2.97}$$

for a scattering event by an angle exceeding some lower limit α^*; (2.97) is a straight application of (2.3). Figure 1.1 on page 4 indicates that for alpha particles, $P(\alpha^*)$ must be a small number ($\ll 1$) if α^* exceeds a few degrees. Therefore, in situations like this the distribution $F(\alpha) \times 2\pi\alpha \mathrm{d}\alpha$ of projectiles after passage through a layer Δx must approach the single-event limit

$$F(\alpha) \Rightarrow N\Delta x K(\alpha) \tag{2.98}$$

for $\alpha \gg \alpha^*$. A rough estimate of the limiting angle α^* is given by the angle which makes the probability (2.97) equal to unity, i.e.,

$$N\Delta x \int_{\phi > \alpha^*} \mathrm{d}\sigma = 1. \tag{2.99}$$

This may be taken to set a limit between single and multiple scattering; it is seen that α^* as given by (2.99) depends on the thickness Δx: The larger Δx the larger α^*.

As a first approximation the following qualitative shape (Fig. 2.7) arises for the multiple-scattering distribution F(α). At angles $\alpha \ll \alpha^*$, where many

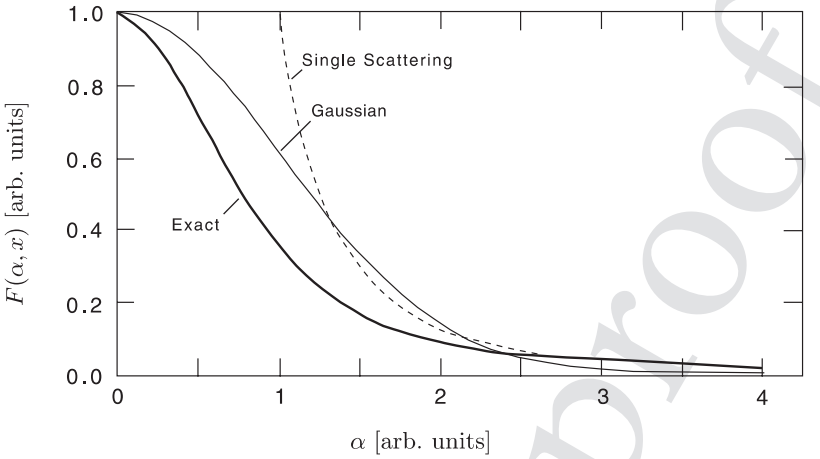

Fig. 2.7. Multiple scattering distribution for heavy projectiles in the model of Williams (1940). Units refer to a quantitative model to be discussed in Volume II. See text

individual deflections contribute to the final value of F(α), one may assume a Gaussian profile with a width given by (2.95)

$$\langle \alpha^2 \rangle = N \Delta x \int_{\phi < \alpha^*} \phi^2 d\sigma; \tag{2.100}$$

in the opposite end, at angles $\alpha \gg \alpha^*$, (2.98) holds.

The above treatment which dates back to Williams (1940) gives a first qualitative orientation. It is often quite reliable. However, a more comprehensive treatment is available and will be discussed in Volume II.

2.4.3 Nuclear and Electronic Scattering

The present section serves the purpose of providing a qualitative estimate of the relative significance of nuclear and electronic collisions in multiple scattering. The treatment will follow that of energy loss in Sect. 2.2.3 on page 33.

The angle of deflection ϕ at impact parameter p follows from the momentum transfer

$$\phi \sim \frac{\Delta P_\perp}{m_1 v} = \sqrt{\frac{m_2 T}{m_1 E}} \tag{2.101}$$

by means of (2.45). Therefore (2.95) reads

$$\langle \alpha^2 \rangle = N \Delta x \int \frac{m_2 T}{m_1 E} \, \mathrm{d}\sigma = \frac{m_2}{m_1 E} \langle \Delta E \rangle, \tag{2.102}$$

where $\langle \Delta E \rangle$ is given by (2.19), or $\langle \Delta E \rangle = N \Delta x S$. Equation (2.102) holds for one target species at a time, i.e., the nuclear and electronic contributions read

$$\langle \alpha^2 \rangle_{\mathrm{n}} = \frac{M_2}{m_1 E} \langle \Delta E \rangle_{\mathrm{n}} \tag{2.103}$$

and

$$\langle \alpha^2 \rangle_{\mathrm{e}} = \frac{m}{m_1 E} \langle \Delta E \rangle_{\mathrm{e}}, \tag{2.104}$$

respectively. These rough estimates – which ignore the upper limit α^* that was introduced in (2.97) – show that the ratio of nuclear to electronic multiple-scattering widths is of the order of

$$\frac{\langle \alpha^2 \rangle_{\mathrm{n}}}{\langle \alpha^2 \rangle_{\mathrm{e}}} \sim Z_2 \frac{L_{\mathrm{n}}}{L_{\mathrm{e}}} \tag{2.105}$$

by means of (2.58).

For heavy target atoms where $Z_2 \gg 1$, the *nuclear* contribution dominates clearly. Moreover, the nuclear stopping number L_{n} normally exceeds the electronic one when the projectile is an ion or another heavy particle – because of the large difference between $(T_{\max})_{\mathrm{n}}$ and $(T_{\max})_{\mathrm{e}}$. This results in a predominantly nuclear multiple-scattering distribution even when the target is light.

The situation is even clearer in the limit of single collisions, $\alpha \gg \alpha^*$. Since the momentum transferred to an electron in a single collision cannot exceed $2mv$ a heavy projectile can be scattered from an electron at most by an angle $\sim 2m/M_1$. This angle – less than 0.1 degree – is frequently within the multiple-scattering limit α^*. Hence, single scattering of heavy projectiles ($m_1 \gg m$) is determined by *nuclear* contributions with the exception of extremely small scattering angles. Another exception is the case of channeling (Fig. 1.3 on page 6) where nuclear scattering events are suppressed.

Let us finally write down the scattering cross section in the small-angle approximation. According to (2.42) and (2.91) we have

$$\phi \sim \frac{|e_1 e_2|}{pE} \tag{2.106}$$

and therefore

$$\mathrm{d}\sigma \sim \left| \frac{\mathrm{d}(\pi p^2)}{\mathrm{d}\phi} \right| \sim \frac{e_1^2 e_2^2}{E^2} \frac{2\pi\phi \mathrm{d}\phi}{\phi^4}. \tag{2.107}$$

In the single-collision limit the probability for a scattering event $(\alpha, \mathrm{d}\alpha)$ is then determined by (2.98), i.e.,

$$F(\alpha_1)\, 2\pi\alpha \mathrm{d}\alpha \simeq N \Delta x\, 2\pi \frac{e_1^2 e^2}{E^2} Z_2^2 \frac{\mathrm{d}\alpha}{\alpha^3} \tag{2.108}$$

for $2m/m_1 \leq \alpha \ll 1$, where $Z_2 e$ is the nuclear charge. For $\alpha \leq 2m/M_1$, target electrons contribute to the scattering cross section. In that case the factor Z_2^2 due to the target charge is to be replaced by Z_2 since there are Z_2 electrons per nucleus. Hence, the effective scattering cross section due to both nuclei and electrons reads

$$\mathrm{d}\sigma \simeq \frac{e_1^2 e^2 Z_2(Z_2+1)}{E^2} \, \frac{2\pi\phi \mathrm{d}\phi}{\phi^4} \tag{2.109}$$

for $\alpha < 2m/m_1$.

The treatment presented here applies to the nonrelativistic regime as it stands. Extension to the relativistic regime is straightforward since the central quantity, the transverse momentum transfer (2.42) is unaffected by relativity. Therefore, the only noticeable change at this level is the replacement of the projectile momentum $m_1 v$ in (2.101) by $m_1 \gamma_v v$, i.e.,

$$m_1 \to \gamma_v m_1 \tag{2.110}$$

in all relations on small-angle multiple scattering.

2.5 Estimates

2.5.1 Alpha Particles

Now let us interpret the qualitative features of the cloud-chamber photograph shown in Fig. 1.1 on page 4. Within the spirit of this chapter we do not aim at high accuracy but rather try to find simple order-of-magnitude estimates.

Start with the range. It is found by insertion of the electronic stopping cross section (2.60) into (2.36) and integrating. This yields very roughly

$$R \sim \frac{mE^2}{M_1 \, 4\pi N Z_2 e_1^2 e^2} \left\{ \frac{1}{L_\mathrm{e}} \right\}, \tag{2.111}$$

where the brackets indicate an average over the trajectory. Note that L_e varies rather slowly with E.

Next get an order-of-magnitude estimate of the range straggling from (2.38) which reads

$$\frac{\Omega_R^2}{R^2} \sim \frac{2m}{M_1} \frac{\{L_\mathrm{e}^{-3}\}}{\{L_\mathrm{e}^{-1}\}^2}; \tag{2.112}$$

This shows that $\Omega_R/R \sim 10^{-2}$ for alpha particles, a result that is consistent with Fig. 1.1 and shows that the continuous-slowing-down-approximation is quite accurate in this case.

Next get an order-of-magnitude estimate of the multiple-scattering angle by setting $\Delta x = R$ in (2.103), i.e., look at the angular spread of an initially well-collimated beam over the entire trajectory,

$$\langle \alpha^2 \rangle = \frac{mZ_2}{2M_1} \left\{ \frac{L_\mathrm{n}}{L_\mathrm{e}} \right\}. \tag{2.113}$$

It is seen that whatever the accurate value of the weighted average $\{L_\mathrm{n}/L_\mathrm{e}\}$, the factor $mZ_2/2M_1 \sim Z_2/15000$ will make sure that $\langle \alpha^2 \rangle$ is a small quantity for an alpha particle. This explains why visible portions of the particle tracks in Fig. 1.1 are essentially straight lines.

Finally, according to (2.108) for $\Delta x = R$, the probability for a large-angle scattering event over the entire trajectory is of the order of

$$NR\,\frac{\pi e_1^2 e^2 Z_2^2}{E^2} \sim \frac{mZ_2}{16M_1} \left\{ \frac{1}{L_\mathrm{e}} \right\}. \tag{2.114}$$

This shows that even for heavy target nuclei only a minute fraction, less than 10^{-2} of the alpha particles, will undergo a major deflection over the main part of their range.

2.5.2 Preview: Energy and Z_1 dependence

Figure 2.8 gives you an impression of what we have learned so far and where we are going. Theoretical stopping cross sections for H, Ar and U ions in Si, found from reliable sources, have been plotted over a wide range of beam energies. All stopping cross sections show the characteristic v^{-2} dependence, modified by the logarithmic variation of the stopping number at high but nonrelativistic energies. In that energy regime, S_n lies more than three orders of magnitude below S_e.

However, both S_e and S_n go through maxima at lower energies and then decrease according to some power-law dependence on the beam energy. Evidently, such maxima must exist, because a particle cannot lose more than its total kinetic energy, but their locations differ dramatically, and no easy estimate of their location and height emerges from what we have learned up till now.

For both Ar and U, there is a low-energy regime where S_n dominates, while this is not expected for hydrogen ions. The height of the maximum in S_e varies over almost three orders of magnitude from H to U, but note that the factor is signifcantly smaller than 92^2, the ratio of the respective values of Z_1^2.

Also, note that S_e starts to increase again at relativistic energies, ~ 1 GeV. The importance of relativistic collision kinematics was recognized right from the beginning (Bohr, 1915).

Finally, experimental data from ~ 25 different sources have been included in case of H-Si, a comparatively well-studied ion-target combination. You may note that at energies above the peak position there is excellent agreement both between different sets of experimental data and between experiment and theory. Discrepancies occur at lower speeds.

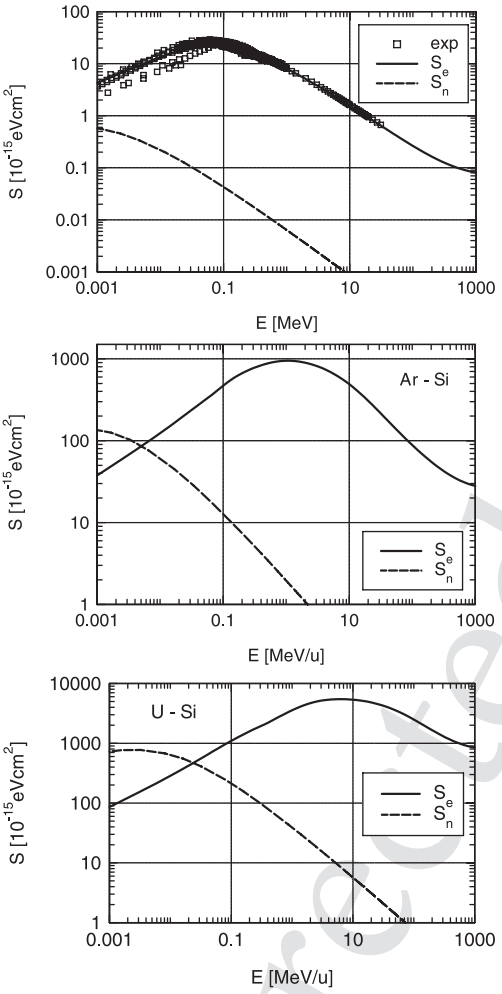

Fig. 2.8. Electronic and nuclear stopping cross sections for H in Si, Ar in Si and U in Si versus beam energy per nucleon. S_n evaluated according to Lindhard et al. (1968). S_e from ICRU (1993) for H-Si, from ICRU (2005) for Ar-Si and for U-Si computed from binary theory (Sigmund and Schinner, 2002). Experimental data from numerous sources compiled by Paul (2005). Note the different abscissa scales

2.6 Electron and Positron Penetration

Several of the explicit results quoted above for stopping and scattering parameters have been derived for projectile masses exceeding the electron mass, i.e., for ions, mesons etc. This implies that the maximum energy transfer to a target electron is close to $2mv^2$ according to (2.61). This does not apply to a positron where the maximum energy transfer is

$$T_{\max} = \frac{m}{2}v^2. \tag{2.115}$$

However, it does not make much sense to insert this into (2.64), because the classical scheme has a very limited range of validity. Instead, we just note that

the stopping force on a positron is smaller than that on a proton at the same projectile speed.

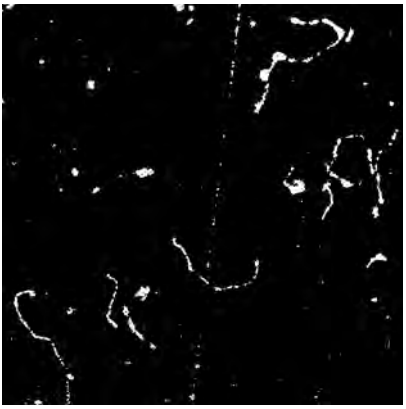

Fig. 2.9. Trajectories of beta particles. From Gentner et al. (1954)

For penetrating electrons a further complication is caused by the indistinguishability of a scattered projectile electron from an ejected target electron in case of substantial energy transfer. In applications of particle penetration theory it is then necessary to consider the possible effects of *both* electrons emerging from a collision. The stopping force is, then, no longer defined in a strict sense. On a less rigorous basis, one may define the mean energy loss as the difference between the initial electron energy and the mean energy of an electron emerging with energy greater than $E/2 = mv^2/4$ from an interaction, i.e.,

$$S = \int_{T_{\min}}^{E/2} T \mathrm{d}\sigma(T) + \int_{E/2}^{E} (E - T) \mathrm{d}\sigma(T). \tag{2.116}$$

This may be rewritten in the form

$$S = \int_{T_{\min}}^{E} T \mathrm{d}\sigma(T) + \int_{E/2}^{E} (E - 2T) \mathrm{d}\sigma(T) \tag{2.117}$$

or, for Coulomb scattering,

$$S_{\text{electron}} = \frac{4\pi Z_2 e^4}{mv^2} \left(L_{\text{positron}} + \frac{1}{2} - \ln 2 \right) \tag{2.118}$$

Electrons and positrons behave dramatically differently from heavy particles with regard to angular deflection. This is most easily seen from (2.113) and (2.114) where replacement of the heavy projectile mass M_1 by m in the denominators implies an increase by a factor of $\gtrsim 2000$ in both $\langle \alpha^2 \rangle$ and the mean number of large-angle scattering events over the length R of the trajectory. This means that the slowing down of electrons and positrons is much

like a diffusive motion. This is illustrated in Fig. 2.9 which differs qualitatively from Fig. 1.1 on page 4. The origin of this difference is the long range of an electron or positron compared with that of a heavy particle *at the same energy*, while the scattering probabilities over a given track length are comparable. If this appears puzzling, it might help to note that the stopping force depends on the projectile *speed* while the cross section for angular deflection depends on the *energy*.

Finally, note that collisions with electrons may give rise to substantial angular deflection, unlike what was found for heavy projectiles. Therefore the expression (2.109), valid only at very small scattering angles for heavy projectiles, has a much wider range of validity for electrons or positrons. It is, however, still a small-angle formula.

2.7 Discussion and Outlook

It may be appropriate at this stage to summarize points where the theory as outlined up till now needs improvement.

Most of all, the arguments presented in Sects. 2.3.4 and 2.3.6 indicate that an evaluation of the electronic stopping force on the basis of a classical electron theory is questionable, at least at high velocities and for low-charge projectiles. Bethe's theory, which will be discussed in Chapter 4, avoids several oversimplifications that entered the estimates discussed above. In particular the incorporation of electronic binding, discrete electron states, zero-point motion of electrons, and the interaction between electrons within a target atom or molecule are all effects that at least in principle are taken fully and properly into account in a quantum theory of the interaction between a moving point charge and an atom or molecule.

Next, from the treatment in Sect. 2.3.4 it follows that a penetrating charged particle effectively interacts with target electrons up to a distance equal to Bohr's adiabatic radius, (2.62). Thus, in condensed matter, even at moderately high speed, the projectile may simultaneously interact with a large number of electrons, i.e., the medium may experience substantial polarization. It is to be expected that a proper theory of charged-particle stopping has to account for collective excitations, in particular so for high-speed particles and in dense matter such as solids and liquids.

With increasing projectile speed various relativistic effects cannot be ignored. Although the basic theory is a straight extension of what has been described in Sects. 2.3.3 and 2.3.4 (Bohr, 1915), the topic has been postponed to Chapters 5 and 6 for stopping and Volume II for scattering.

More complex are those effects that originate in the fact that moving particles need not be point charges, especially ions at moderate and low velocities. Indeed, ions with high atomic numbers are usually not fully stripped, and the interaction of an ion carrying an electron cloud with the atoms of the stopping medium can be quite complex, in particular at velocities near or below the

orbital velocities of target electrons. The quantum state of a moving ion may undergo changes during a passage, and electron capture and loss processes add to the complexity of the problem. An attempt to discuss some of these problems will be postponed to Volume II when a number of prerequisites will be available.

Nuclear collisions have been treated in a very rough manner in this chapter and mainly from the point of view of its implications to multiple scattering. The reader may have recognized from the discussion in Sect. 2.3.7 that the truncation of nuclear stopping becomes effective at velocities far below those where electronic stopping drops off. This indicates that nuclear stopping dominates at the lowest velocities, but even an order-of-magnitude estimate of this effect requires a more careful discussion of atomic screening. Nuclear scattering and stopping will be studied in Volume II.

Some of the statistical aspects of particle penetration need clarification and specification. The practical limits to Poisson statistics are not clear at this point. In particular it is not obvious to what extent a disordered solid or a liquid can be regarded as a gas at high pressure with respect to the stopping and scattering of ions. Information is needed on the shape of energy-loss and multiple-scattering distributions, and some statistical information on the combined effect of stopping and scattering is desirable. The conditions for separation of electronic from nuclear stopping and scattering are not clear. Finally, the statistics of ion ranges needs to be discussed.

Problems

2.1. The mean number $\langle n \rangle$ of ionizations produced by an alpha particle slowing down to rest from an initial energy E is given with good accuracy by the expression[9] $\langle n \rangle = E/W$, where W is a measure of the energy spent in the creation of an ion pair, i.e., a free electron and a positive ion. W is always greater than the first ionization potential (why?). For atmospheric air, it is empirically given as $W = 29.6$ eV (ICRU, 1979). Find $\langle n \rangle = E/W$ for the case depicted in Fig. 1.1 on page 4 and give a rough estimate of the number of ions produced per micrometer travelled pathlength.

2.2. Repeat the derivation of (2.1–2.3) in the reverse order by starting at (2.3).

2.3. Consult your favored textbooks in classical and quantum mechanics on how they define cross sections and try to reconcile this with the arguments that lead to (2.1–2.3). Most discussions in textbooks refer to particular processes and lead to only one of the three relations.

2.4. Verify the validity of (2.8–2.10) and derive corresponding relations for the cumulants $\overline{(n - \langle n \rangle)^\nu}$ for $\nu = 3, 4, 5$.

[9] This formula will be derived in Volume III.

2.5. The expression

$$\frac{\left\langle (n - \langle n \rangle)^2 \right\rangle^{1/2}}{\langle n \rangle} \tag{2.119}$$

is sometimes called the relative width of a distribution. The ratio

$$\frac{\left\langle (n - \langle n \rangle)^3 \right\rangle}{\left\langle (n - \langle n \rangle)^2 \right\rangle^{3/2}} \tag{2.120}$$

is called the skewness, and the ratio

$$\frac{\left\langle (n - \langle n \rangle)^4 \right\rangle}{\left\langle (n - \langle n \rangle)^2 \right\rangle^2} \tag{2.121}$$

is called the curtosis. Determine all three quantities for the Poisson distribution.

2.6. Apply a graphics program to generate plots of the Poisson distribution for $0.01 < \langle n \rangle < 100$ at reasonable intervals. Also include gaussian distributions with mean value and variance both given by $\langle n \rangle$ and draw conclusions from the degree of agreement.

2.7. Try to estimate the variance in the number of ionizations made by an alpha particle, referring to Fig. 1.1 and Problem 2.1, assuming Poisson-like distribution. Your result *overestimates* the fluctuation. We shall see in volume III that the distribution is non-poissonian and that the variance is reduced by a numerical factor, the 'Fano factor'.

2.8. Extract an order-of-magnitude estimate for the stopping cross section of an alpha particle from Fig. 1.1 by assuming S to be energy-independent.

2.9. Use (2.36) in conjunction with Fig. 1.1 to estimate the range of an alpha particle in liquid air.

2.10. Extract an order-of-magnitude estimate of Ω_R^2 from Fig. 1.1, use the result of problem 2.9 to extract an order-of-magnitude value of W, and compare your result with the appropriate predictions given in Sect. 2.3.3.

2.11. Determine values of the following quantities in gaussian units,

- an electric field of 1 V/m,
- a voltage of 1 V,
- a magnetic field of 1 T,
- a charge of 1 C and
- a current of 1 A,

2.12. Write down Rutherford's law for the scattering of two point charges on each other in

– SI units,
– gaussian units and
– atomic units.

2.13. Derive a criterion for the range of validity of (2.42) by estimating the pathlength travelled by the hit particle during the collision time τ, assuming constant acceleration in accordance with $F_{\max}$. Require that pathlength to be small compared to the impact parameter.

2.14. You will most likely be unable to find (2.47) in your classical-mechanics text[10]. Instead of the energy transfer T, the running variable is usually the center-of-mass scattering angle Θ. Find the relation between the two variables and the relation between the two corresponding differential cross sections[11].

2.15. Equation (2.45) is an approximate form of an exact relation which, in terms of the center-of-mass scattering angle Θ instead of T, is derived in standard textbooks of classical mechanics. Locate the exact relation in your favored text and use the result of problem 2.14 to transform it into $T = T(p)$. Find out which quantity you have to assume small in order to arrive at (2.45) as a limit, and verify that this is consistent with what has been assumed in the derivation of (2.45).

2.16. Derive (2.47) from the exact relation $T = T(p)$ which you found in problem 2.15 and identify the reason why both the approximate and the exact relation lead to the same differential cross section.

2.17. Verify the validity of each of (2.48 - 2.50) either by consulting a classical-mechanics text or by writing down conservation laws of energy and momentum for a linear collision.

2.18. Referring to Fig. 2.4, try to analyse how the projectile can slow down, i.e., lose momentum in the beam direction, despite the fact that momentum is transferred to the target electron perpendicular to its velocity.

2.19. Make a model to illustrate the adiabatic limit by explicitly evaluating the energy transferred to a linear classical harmonic oscillator by a force $F(t)$ of some adopted shape. Try a) a simple pulse with $F = \text{const}$ over some time interval τ, b) a triangular pulse, c) a lorentzian, and d) a gaussian. Use the Green function of the classical harmonic oscillator. If you are unfamiliar with this concept, consult Appendix A.2.5 first or check (4.6) in chapter 4. Express all results in terms of the transferred momentum $\int_{-\infty}^{\infty} F(t)dt$ to a free electron, define appropriate effective collision times, and compare the results.

[10] A notable exception is the book of Landau and Lifshitz (1960).
[11] The reader who has difficulties solving problems 2.14–2.17 may wish to study Chapter 3 first.

2.20. Go carefully through the various steps leading to (2.79). Try to generalize the estimate by adopting an arbitrary relation between the scattering angle $\phi(p)$ of the projectile in the laboratory system and the impact parameter.

2.21. Use three-dimensional graphics to illustrate (2.80). Include the limit expressed by (2.83).

2.22. Check a few texts on quantum theory and atomic physics for what they write about screening. Find expressions for the electron density as a function of the distance from the nucleus. If necessary, take an average over the angular variables. Extract representative values of the screening radius a.

2.23. Devise a simple estimate showing that $\hbar\omega_0$ for typical vibrational frequencies in molecules lies in the range around or below 0.1 eV, as mentioned in the beginning of Sect. 2.3.7.

2.24. Derive (2.85) from the results of Sect. 2.3.6.

2.25. Go explicitly through the steps leading to (2.93) and (2.94) and make sure that no other complications arise from the vectorial nature of the scattering angles than those mentioned in the text.

2.26. The cross sections listed in the end of Sect. 2.4.3 are all divergent at small angles. Verify that these divergencies are equivalent with the $1/T^2$ divergence of the Rutherford cross section expressed as a function of energy transfer. What is it that causes an integral like (2.100) to converge at small angles?

2.27. Verify (2.115).

2.28. Discuss qualitatively possible differences between electrons and positrons regarding scattering and stopping.

References

Bohr N. (1913): On the theory of the decrease of velocity of moving electrified particles on passing through matter. Philos Mag **25**, 10–31

Bohr N. (1915): On the decrease of velocity of swiftly moving electrified particles in passing through matter. Philos Mag **30**, 581–612

Bohr N. (1948): The penetration of atomic particles through matter. Mat Fys Medd Dan Vid Selsk **18 no. 8**, 1–144

Bonderup E. (1981): *Interaction of charged particles with matter*. Institute of Physics, Aarhus

Bragg W.H. and Kleeman R. (1905): On the alpha particles of radium, and their loss of range in passing through various atoms and molecules. Philos Mag **10**, 318–341

Darwin C.G. (1912): A theory of the absorption and scattering of the α rays. Phil Mag (6) **23**, 901–921

Feller W. (1968): *An introduction to probability theory and its applications*, vol. I. J. Wiley and Sons, London

Gentner W., Mayer-Leibnitz H. and Bothe W. (1954): *Atlas of typical expansion chamber photographs*. Pergamon Press, London

Gordon W. (1928): Über den Stoß zweier Punktladungen nach der Wellenmechanik. Z Physik **48**, 180–191

ICRU (1979): *Average energy to produce an ion pair*, vol. 31 of *ICRU Report*. International Commission of Radiation Units and Measurements, Bethesda, Maryland

ICRU (1993): *Stopping powers and ranges for protons and alpha particles*, vol. 49 of *ICRU Report*. International Commission of Radiation Units and Measurements, Bethesda, Maryland

ICRU (2005): *Stopping of ions heavier than helium*, vol. 73 of *ICRU Report*. Oxford University Press, Oxford

Landau L. and Lifshitz E.M. (1960): *Mechanics*, vol. 1 of *Course of theoretical physics*. Pergamon Press, Oxford

Leithäuser G.E. (1904): Über den Geschwindingkeitsverlust, welchen die Kathodenstrahlen beim Durchgang durch dünne Metallschichten erleiden. Ann Physik **15**, 283–306

Lindhard J., Nielsen V. and Scharff M. (1968): Approximation method in classical scattering by screened Coulomb fields. Mat Fys Medd Dan Vid Selsk **36 no. 10**, 1–32

Paul H. (2005): Stopping power graphs. URL `www.exphys.uni-linz.ac.at/stopping/`

Rutherford E. (1911): The scattering of alpha and beta particles by matter and the structure of the atom. Philos Mag **21**, 669–688

Sigmund P. (2000): Stopping power: Wrong terminology? ICRU News **1**, 5–6

Sigmund P. and Schinner A. (2002): Binary theory of electronic stopping. Nucl Instrum Methods B **195**, 64–90

Sklodowska-Curie M. (1900): Sur la penetration des rayons de Becquerel non deviables par le champ magnetique. Compt Rend Acad Sci **130**, 76–79

v. Smoluchowski M. (1904): Über Unregelmäßigkeiten in der Verteilung von Gasmolekülen und deren Einfluß auf Entropie und Zustandssume. In *Festschrift Ludwig Boltzmann*, 626–641

Thomson J.J. (1912): Ionization by moving electrified particles. Philos Mag **23**, 449–457

Williams E.J. (1940): Multiple scattering of fast electrons and alpha-particles, and "curvature" of cloud tracks due to scattering. Phys Rev **58**, 292–306

Williams E.J. (1945): Application of ordinary space-time concepts in collision problems and relation of classical theory to Born's approximation. Rev Mod Phys **17**, 217–226